DOI: 10.1002/ejoc.200901157

Cu^{I}-Catalyzed Azide–Alkyne Intramolecular *i*-to-(*i*+4) Side-Chain-to-Side-Chain Cyclization Promotes the Formation of Helix-Like Secondary Structures

Mario Scrima,[a] Alexandra Le Chevalier-Isaad,[b,c] Paolo Rovero,[b,d] Anna Maria Papini,[b,c] Michael Chorev,[e,f] and Anna Maria D'Ursi*[a]

Keywords: Cyclopeptides / Helical structures / Conformation analysis / Click chemistry / Human parathyroid hormone-related protein

A solid-phase assembly of model peptides derived from human parathyroid hormone-related protein (11–19) containing ω-azido- and ω-yl-α-amino acid residues in positions *i* and *i*+4 was cyclised in solution by an intramolecular Cu^{I}-catalyzed azide–alkyne 1,3-dipolar Huisgen cycloaddition. These series of heterodetic cyclo-nonapeptides varied in the size of the disubstituted 1,2,3-triazolyl-containing bridge, the location and the orientation of the 1,2,3-triazolyl moiety within the bridge. The 1,2,3-triazolyl moiety, presented at either 1,4- or 4,1-orientation, is flanked by side chains containing 1–4 CH_2 groups that result in bridges comprised from 4–7 CH_2 groups connecting residues 13 and 17. Comprehensive conformational analysis employing CD, NMR and molecular dynamics reveals the conformational propensities of these heterodetic cyclo-nonapeptides. Cyclo-nonapeptides containing either the 7 methylene bridge (**VII** and **VIII**) or the 4 methylene bridge (**II**) are unstructured in structure-promoting solvent. Cyclo-nonapeptide **I** in which the 1,4-disubstituted 1,2,3-triazolyl is flanked by 3 and 1 CH_2 groups in proximity to the respective residues 13 and 17, is stabilized in a non-canonical structure. All the other heterodetic cyclo-nonapeptides (**III**–**VI**) in which the 1,2,3-triazolyl is flanked by a total of 5 or 6 CH_2 groups nicely accommodate α-helical structures and reproduce very closely the helical structure stabilized by the analogous cyclo-nonapeptide in which Lys^{13} and Asp^{17} are bridged by the isosteric lactam. These studies suggest that the bioorthogonal *i*-to-(*i*+4) side-chain-to-side-chain cyclization via the prototypic "click reaction" offers a new and powerful approach for generating stable helix mimetic structures.

Introduction

At the macromolecular interacting sites found in receptors, enzymes, channels, and protein-protein interfaces peptide ligands assume well-defined conformations that recognize, bind and trigger specific biological responses. However, in solution, linear peptides exist as ensembles of conformers in dynamic steady-state equilibrium. Side-chain-to-side-chain cyclizations through intramolecular covalent bond formation represent a frequently practiced strategy to stabilize the so called bioactive conformations, which may contribute to enhanced potency, improved target selectivity, favourable pharmacokinetic properties, and increased metabolic stability.

[a] Dipartimento di Scienze Farmaceutiche,
via Ponte Don Melillo 11C, 84084 Salerno, Italy
Fax: +39-089-969602
E-mail: dursi@unisa.it
[b] Laboratory of Peptide & Protein Chemistry & Biology, Polo Scientifico e Tecnologico, University of Firenze,
50019 Sesto Fiorentino, Italy
[c] Dipartimento di Chimica Organica, Polo Scientifico e Tecnologico, University of Firenze,
via della Lastruccia 13, 50019 Sesto Fiorentino, Italy
[d] Dipartimento di Scienze Farmaceutiche, University of Firenze, via Ugo Schiff 3, Polo Scientifico e Tecnologico, 50019 Sesto Fiorentino, Italy
[e] Laboratory for Translational Research, Harvard Medical School,
One Kendal Square, Building 600, Cambridge, Massachusetts 02139, USA
[f] Department of Medicine, Brigham and Women's Hospital,
75 Francis Street, Boston, MA 02115, USA

Supporting information for this article is available on the WWW under http://dx.doi.org/10.1002/ejoc.200901157.

Abbreviations: Boc: *tert*-butyloxycarbonyl, CD: circular dichroism, DCM: dichloromethane, DMF: *N*,*N*-dimethylformamide, DQF-COSY: double quantum-filtered correlation spectroscopy, ESCI-MS: electrospray/chemical ionization mass spectra, Fmoc: 9-fluorenylmethoxycarbonyl, HFA: hexafluoroacetone, HFIP: hexafluoro-2-propanol, HOBt: *N*-hydroxybenzotriazole, HPLC: high-performance liquid chromatography, MD: molecular dynamics, NMM: *N*-methylmorpholine, NOE: nuclear Overhauser effect, NOESY: NOE spectroscopy, Pbf: (2,2,4,6,7-pentamethyldihydrobenzofuran-5-yl)sulfonyl, PTHR1: parathyroid hormone receptor 1, PTHrP: parathyroid hormone-related peptide, RMSD: root mean square deviation, RP-HPLC: reversed-phase HPLC, t_R: retention time, SPPS: solid-phase peptide synthesis, TBTU: 2-(1*H*-benzotriazol-1-yl)-1,1,3,3-tetramethyluronium tetrafluoroborate, TFA: trifluoroacetic acid, TFE: trifluoroethanol, TOCSY: Total Correlated Spectroscopy, Trt: trityl, UPLC: ultra-performance liquid chromatography.

Intramolecular side-chain-to-side-chain cyclizations through bridges include those formed by the redox susceptible and hydrophobic disulfide bonds between pairs of cysteines,[2] the polar lactams between pairs of ω-amino- and ω-carboxyl-α-amino acids,[3] and the all hydrophobic "stapled" rings between pairs of non-coded ω-olefin-derivatized α-amino acids.[4] To enable unambiguously targeted intramolecular side-chain-to-side-chain disulfide- and lactam-bridged cyclizations, orthogonal protection strategies are employed. Moreover, insertion of cysteines or non-biogenic amino acids such as ω-alkenyl-α-amino acid residues leads to highly hydrophobic bridges (e.g. disulfide and olefin bridges).[5] Evidently, side-chain-to-side-chain cyclization via amide bond isosteres that can be carried out without elaborated orthogonal protection schemes is of interest and will fulfil important unmet needs. To this end, the recently introduced Cu^{I}-catalyzed azide–alkyne 1,3-dipolar cycloaddition, a prototypic "click chemistry" reaction,[6–8] presents an interesting opportunity to develop a new paradigm for generating heterodetic cyclopeptides through pseudopeptidic and bioorthogonal intramolecular side-chain-to-side-chain cyclization. The inherent low reactivity of the azide and alkynyl functions toward an expansive range of functional groups and reagents eliminates the need for elaborate protection schemes. In addition, the 1,4-disubstituted 1,2,3-triazolyl bridging moiety which is isosteric to the lactam bridge is also inert toward a vast variety of synthetic conditions and its proteolytic stability is of great importance for applications in biological and material sciences.[6,8–13]

Recently, we have reported on different approaches to synthesize a model *i*-to-(*i*+4) side-chain-to-side-chain 1,4-disubstituted 1,2,3-triazolyl-bridged cyclo-nonapeptide [N^{α}-Ac-Lys-Gly-Xaa(&^{1})-Ser-Ile-Gln-Yaa(&^{2})-Leu-Arg-NH_2]-[{&^{1}}$(CH_2)_4$-1,4-(1,2,3)triazolyl-CH_2&^{2}}] derived from parathyroid hormone-related peptide (PTHrP)[1] (Scheme 1, III) and compared its conformational preferences with the corresponding *i*-to-(*i*+4) side-chain-to-side-chain lactam-bridged cyclo-nonapeptide, [N^{α}-Ac-Lys-Gly-Lys(&^{1})-Ser-Ile-Gln-Asp(&^{2})-Leu-Arg-NH_2]. Both the heterodetic cyclopeptides III and the corresponding lactam, which is a truncated version of the α-helical and potent parathyroid hormone receptor 1 (PTHR1) agonist [Lys^{13}(&^{1}),Asp^{17}-

Linear precursors		1,4-Disubstituted 1,2,3-triazolyl-containing cyclo-nonapeptides	
I' [a]	N^{α}-Ac-Lys-Gly-Nva(δ-N_3)-Ser-Ile-Gln-Pra-Leu-Arg-NH_2	I	N^{α}-Ac-Lys-Gly-NHCHCO-Ser-Ile-Gln-NHCHCO-Leu-Arg-NH_2
II'	N^{α}-Ac-Lys-Gly-Pra-Ser-Ile-Gln-Nva(δ-N_3)-Leu-Arg-NH_2	II	N^{α}-Ac-Lys-Gly-NHCHCO-Ser-Ile-Gln-NHCHCO-Leu-Arg-NH_2
III' [b]	N^{α}-Ac-Lys-Gly-Nle(ε-N_3)-Ser-Ile-Gln-Pra-Leu-Arg-NH_2	III[b]	N^{α}-Ac-Lys-Gly-NHCHCO-Ser-Ile-Gln-NHCHCO-Leu-Arg-NH_2
IV'	N^{α}-Ac-Lys-Gly-Pra-Ser-Ile-Gln-Nle(ε-N_3)-Leu-Arg-NH_2	IV	N^{α}-Ac-Lys-Gly-NHCHCO-Ser-Ile-Gln-NHCHCO-Leu-Arg-NH_2
V'	N^{α}-Ac-Lys-Gly-hAla(γ-N_3)-Ser-Ile-Gln-Nle(δ-yl)-Leu-Arg-NH_2	V	N^{α}-Ac-Lys-Gly-NHCHCO-Ser-Ile-Gln-NHCHCO-Leu-Arg-NH_2
VI'	N^{α}-Ac-Lys-Gly-Nle(δ-yl)-Ser-Ile-Gln-hAla(γ-N_3)-Leu-Arg-NH_2	VI	N^{α}-Ac-Lys-Gly-NHCHCO-Ser-Ile-Gln-NHCHCO-Leu-Arg-NH_2
VII'	N^{α}-Ac-Lys-Gly-Nva(δ-N_3)-Ser-Ile-Gln-Nle(δ-yl)-Leu-Arg-NH_2	VII	N^{α}-Ac-Lys-Gly-NHCHO-Ser-Ile-Gln-NHCHCO-Leu-Arg-NH_2
VIII'	N^{α}-Ac-Lys-Gly-Nle(δ-yl)-Ser-Ile-Gln-Nva(δ-N_3)-Leu-Arg-NH_2	VIII	N^{α}-Ac-Lys-Gly-NHCHCO-Ser-Ile-Gln-NHCHCO-Leu-Arg-NH_2

[a] Specific nomencluture used throughout this paper: hAla(γ-N_3), γ-azido-L-homoalanyl; Nle(ε-N_3), ε-azido-L-norleucyl; Nle(δ-yl), δ-ethynyl-L-norleucyl; Nva(δ-N_3), δ-azido-L-norvalyl; Pra, L-propargylglycyl.

[b] Compounds **III'** and **III** were previously reported by us[13] and are included for discussion purposes only. ω-Azido-containing α-amino acyl residues and their corresponding fragment in the cyclopeptide are printed in **red** in the left and right columns of the Table, respectively. ω-Ethynyl-containing α-amino acyl residues and their corresponding fragment in the cyclopeptide are printed in **blue** in the left and right columns of the Table, respectively.

Scheme 1. Linear precursors **I′**–**VIII′** (excluding **III′** that was reported previously[1]): linear peptides in which Lys^{13} and Asp^{17} were replaced with ω-azido- and ω-yl-α-amino acid residues. *i*-to-(*i*+4) side-chain-to-side-chain 1,4-disubstituted 1,2,3-triazolyl-bridged cyclo-nonapeptides (**I**–**VIII**, excluding **III** that was reported previously[1]) are derived from the model peptide N^{α}-Ac-PTHrP(11–19)NH_2.

(&²)]PTHrP(1–34)NH_2,[14,15] share the same spatial orientation of the side-chains of Ser, Gln, and Ile located at the *i*+1 to *i*+3 positions of the ring-forming sequences.[13]

Herein we report on the synthesis and a comprehensive conformational analysis of a series of *i*-to-(*i*+4) side-chain-to-side-chain 1,4-disubstituted 1,2,3-triazolyl-bridged cyclo-nonapeptides (Scheme 1, **I**–**VIII**, except **III** that was reported previously)[1] derived from the model peptide N^{α}-Ac-PTHrP(11–19)NH_2. Solid phase peptide synthesis generated a series of linear peptides in which Lys^{13} and Asp^{17} were replaced with ω-azido- and ω-yl-α-amino acid residues (Scheme 1, structures **I′**–**VIII′**, except **III′** that was reported previously).[1,16] Solution phase intramolecular Cu^{I}-catalyzed azide–alkyne 1,3-dipolar Huisgen cycloaddition[6,8] resulted in cyclo-nonapeptides comprised from side-chains bridged by either 1,4- or 4,1-disubstituted 1,2,3-triazolyl moieties (**I**, **III**, **V**, and **VII**, and **II**, **IV**, **VI**, and **VIII**, respectively). The bridging 1,2,3-triazolyl rings are flanked by alkyl chains $(CH_2)_m$ and $(CH_2)_n$ (where $m \neq n$, n and m = 1–4 and $m+n$ = 4, 5, 6, and 7) located at the C^{α} of residues 13 and 17, respectively. Conformational analysis that included circular dichroism (CD) and ^{1}H-nuclear magnetic resonance (NMR) in water and water/hexafluoroacetone (HFA) mixture, and molecular dynamics simulations (MD) revealed the impact of the size of the 1,2,3-triazolyl-containing bridge, the orientation and the position of the 1,2,3-triazolyl moiety within the connecting bridge on the conformational propensities of these heterodetic cyclo-nonapeptides. These results offer an initial set of guidelines for the use of this new class of side-chain-to-side-chain intramolecular cyclization in the rational design of conformationally stabilized peptides important in the development of novel biomaterial and peptide-based drugs.

Results

Synthesis of 1,2,3-Triazolyl-Containing Cyclo-Nonapeptides

Synthesis of Linear Precursors

The assembly of the resin-bound linear peptide precursors **I′** to **VIII′** by TBTU/HOBt/NMM-mediated couplings was carried out in a straightforward manner, by the Fmoc/*t*Bu solid phase peptide synthesis (SPPS) methodology. As previously reported, the incorporation of the building blocks N^{α}-Fmoc-Xaa(ω-N_3)-OH and N^{α}-Fmoc-Yaa(ω-yl)-OH during the SPPS was found to be the most convenient approach to introduce the functions essential for the subsequent solution phase, Cu^{I}-catalyzed intramolecular azide–alkyne cycloaddition.[1]

Cyclization of the Linear Precursors via Intramolecular Click Reaction

HPLC-purified linear peptide precursors **I′** to **VIII′** were subjected to solution-phase intrachain Cu^{I}-catalyzed side-chain-to-side-chain azide–alkyne 1,3-dipolar cycloaddition. The click reaction conditions were identical to those reported by us previously and used 10-fold molar excess of $CuSO_4 \cdot 5H_2O$ and ascorbic acid in *t*BuOH/H_2O (1:2, v/v).[1] Complete and clean conversion of all linear precursors into the desired heterodetic 1,2,3-triazolyl-containing cyclo-nonapeptides **I**–**VIII** was observed. Under these condition there is no formation of oligomeric products resulting from intermolecular click reactions, thus suggesting formation of a Cu^{I}/acetylide/azide complex with high preference for intramolecular cyclizations.[17] In an attempt to identify putative non-catalyzed spontaneous click reaction, leading to intramolecular cyclization or oligomerization, via intermolecular interaction we have incubated the pure linear peptides **I′**–**VIII′** in water pH = 6 at 1 mg/mL for 12 days at room temperature and monitored changes daily, by RP-HPLC and when warranted, also by electrospray ionization (ESI)-MS analyses. At the end of the incubation we were able to detect only traces of the heterodetic 1,2,3-triazolyl-containing cyclo-nonapeptide (0.5%–2.8% relative to the linear precursor) (Figure 1). Only in the case of the linear peptide **III′** we were able to detected the characteristic *m*/*z* = $[M + 3H]^+$ attributed to the formation of the 1,2,3-triazolyl-containing dimer (not shown). Therefore, in the relatively short catalyzed cyclization we can rule out significant contributions from non-catalyzed spontaneous intramolecular cyclizations to the formation of the heterodetic 1,2,3-triazolyl-containing cyclo-nonapetides **I**–**VIII**.

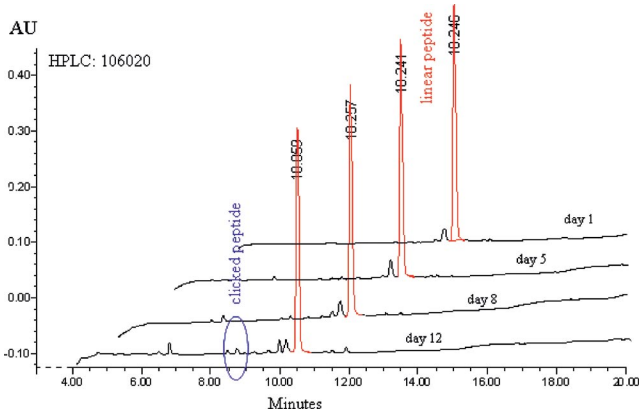

Figure 1. RP-HPLC chromatograms of the linear peptide precursor incubated in *t*BuOH/H_2O (1:2, v/v) in the absence of catalyst. Evolution of the chromatograms during 12 days incubation of linear peptide precursors **I′** in water pH = 6 at 1 mg/mL. The chromatograms were obtained employing a linear gradient of 10% to 60% of B in A for 20 min, A = 0.1% TFA in H_2O, B = 0.1% TFA in CH_3CN.

CD Analysis

A preliminary screening of the conformational preferences of the 1,2,3-triazolyl-containing cyclo-nonapeptides **I**–**II** and **IV**–**VIII** as a function of the solvent system was performed by means of CD spectroscopy.

CD spectra were recorded in water solution and in a water/HFA mixture (1:1, v/v). Figure 2 shows the CD spectra of 1,2,3-triazolyl-containing cyclo-nonapeptides (**I**–**II** and **IV**–**VIII**) recorded in water (pH 6.6) (Figure 2, upper panel) and in water/HFA (1:1, v/v) (Figure 2, lower panel).

Table 1. Quantitative evaluation of the CD spectra using DICHROWEB website (ContinLL). Relative abundance of conformational populations are reported for cyclopeptides **I**–**II** and **IV**–**VIII** recorded in water (pH 6.6) and in HFA/water (1:1, v/v).

Cyclopeptide	Secondary structure							
	Helix		*Strand*		*Turn*		*Disordered*	
	HFA/water	*water*	*HFA/water*	*water*	*HFA/water*	*water*	*HFA/water*	*water*
I	0.900	0.339	0	0.235	0.100	0.298	0	0.128
II	0.800	0.340	0	0.100	0.200	0.330	0	0.230
IV	1	0.524	0	0.05	0	0.196	0	0.230
V	1	0.843	0	0.009	0	0.148	0	0
VI	1	0.553	0	0.040	0	0.279	0	0.128
VII	1	1	0	0	0	0	0	0
VIII	1	0.793	0	0.010	0	0.197	0	0

All CD spectra present the typical shapes of turn-helical structures. The quantitative analysis of CD curves using ContinLL algorithm on DICHROWEB website,[18] (Table 1) shows that cyclo-nonapeptides **I**–**II** and **IV**–**VIII** in water are present in similar proportions of α-helical, turn and random coil conformations, suggesting that in water the cyclo-nonapeptides are characterized by flexible conformations in steady-state equilibrium.

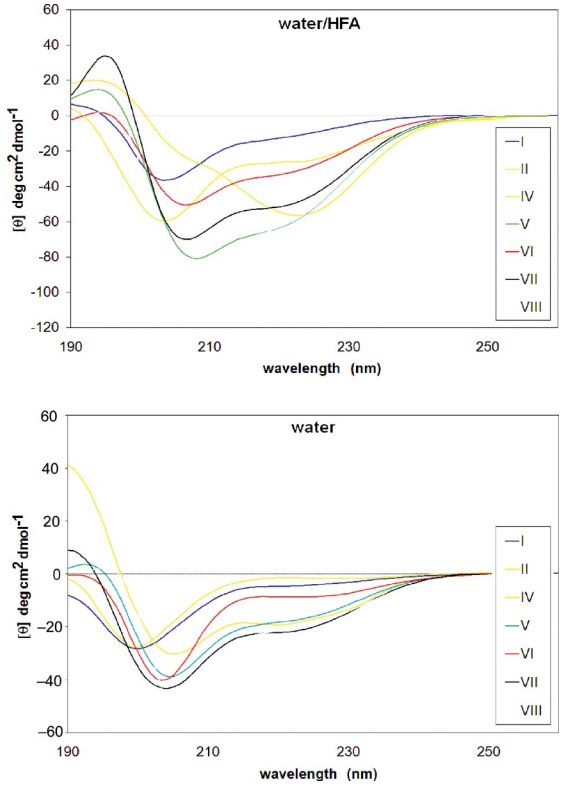

Figure 2. CD spectra of *i*-to-(*i*+4) side-chain-to-side-chain 1,2,3-triazolyl-bridged cyclo-nonapeptides **I**–**II** and **IV**–**VIII** recorded in water (upper-panel) and water/HFA (1:1, v/v) (lower-panel).

In water/HFA mixtures, a prevalent contribution of helical conformations is detectable, indicating the presence of ordered structures.

NMR Analysis

NMR spectra were acquired in water and water/HFA (1:1, v/v), the same solvents used for the CD measurement. To exclude potential aggregation, we recorded the 1D proton spectra of the 1,2,3-triazolyl-containing cyclo-nonapeptides **I**–**II** and **IV**–**VIII** at a concentration range spanning 1.0–0.1 mM. At a peptide concentration of 1.0 mM there were not any noticeable effects of aggregation. Therefore, our NMR analyses were carried at sample concentrations of 0.1 mM. Chemical shift assignments of the proton spectra of 1,2,3-triazolyl-containing cyclo-nonapeptides **I**–**II** and **IV**–**VIII** in water and in water/HFA mixture were achieved via the standard systematic application of DQF-COSY, TOCSY and NOESY experiments,[19–21] using the SPARKY software package[22] according to the procedure of Wüthrich.[23]

The values of the proton chemical shifts for each 1,2,3-triazolyl-containing cyclo-nonapeptide in water and in water/HFA (1:1, v/v), are reported in the Supporting Information Section (Tables S5–S7). These tables also include the chemical shifts differences between Hα values of **I**, **II** and **IV**–**VIII** cyclo-nonapeptides analyzed by us and those reported for random coil conformation.[24] The analysis of chemical shift differences of cyclopeptides in water and water/HFA mixture displays a remarkable up-field Hα chemical shifts as compared to the standard values reported for random coil conformations. This up-field shift, known as indicative of turn-helical structures,[24] supports the conclusion drawn from the CD data on the presence of turn-helical structures for all cyclo-nonapeptides **I**, **II** and **IV**–**VIII** in water as well as in water/HFA solution.

Amide and fingerprint regions of NOESY spectra of **I**, **II** and **IV**–**VIII** cyclo-nonapeptides collected in water, and in water/HFA (1:1, v/v) are reported in Supporting Information Section (Figures S15–S18). Figure 3 and Figure 4 summarize NOE data for 1,2,3-triazolyl-containing cyclo-nonapeptides **I**, **II** and **IV**–**VIII** in water and water/HFA solution, respectively. NOESY spectra of cyclo-nonapeptides in water include few significant NOE connectivities suggesting a low contribution of regular secondary structures. On the contrary, NOESY spectra of cyclo-nonapeptides **I**, **II** and **IV**–**VIII** in water/HFA mixture display a high number of sequential and medium range NOEs. In particular sequential α-N(*i*,*i*+1) and NH-NH(*i*,*i*+1) NOE connectivities, as well as medium range α-N(*i*,*i*+2), NH-NH(*i*,*i*+2) and NH-NH(*i*,*i*+3) NOE connectivities, define patterns which are diagnostic of specific canonical secondary structures.[23]

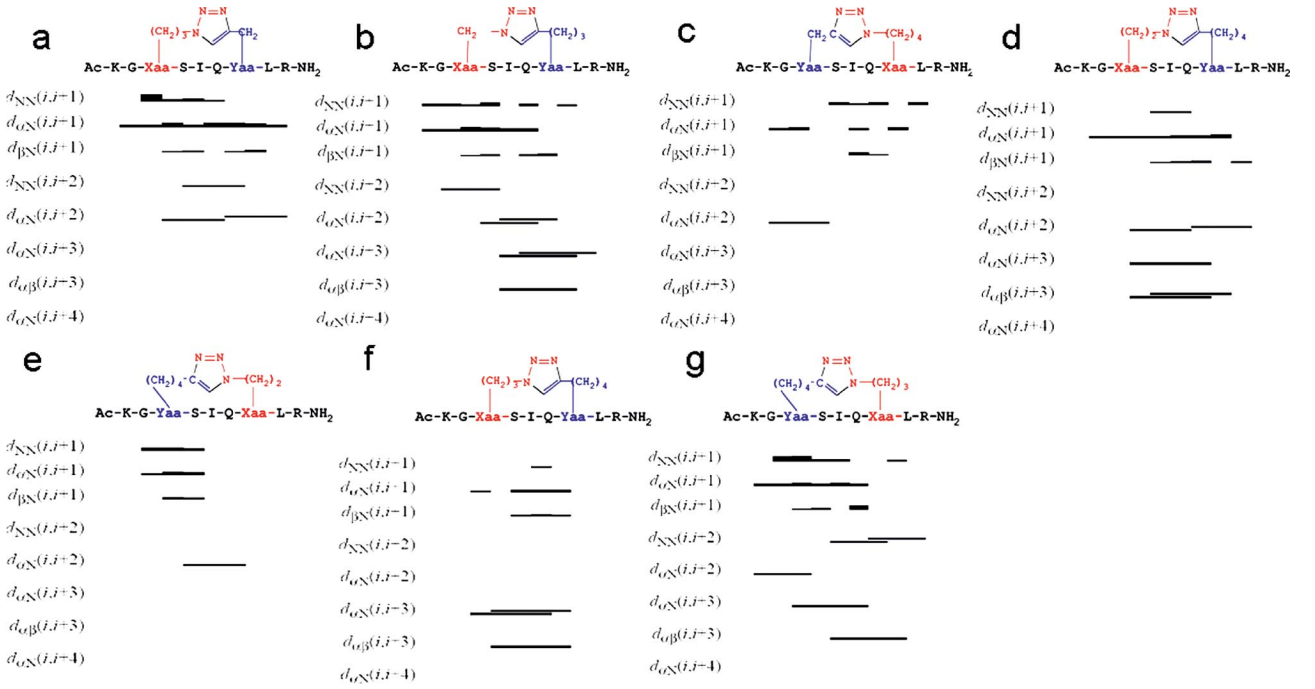

Figure 3. NOE connectivities diagrams of *i*-to-(*i*+4) side-chain-to-side-chain 1,2,3-triazolyl-bridged cyclo-nonapeptide **I**–**II** (panels **a** and **b**) and **IV**–**VIII** (panels **c**–**g**) in water solution.

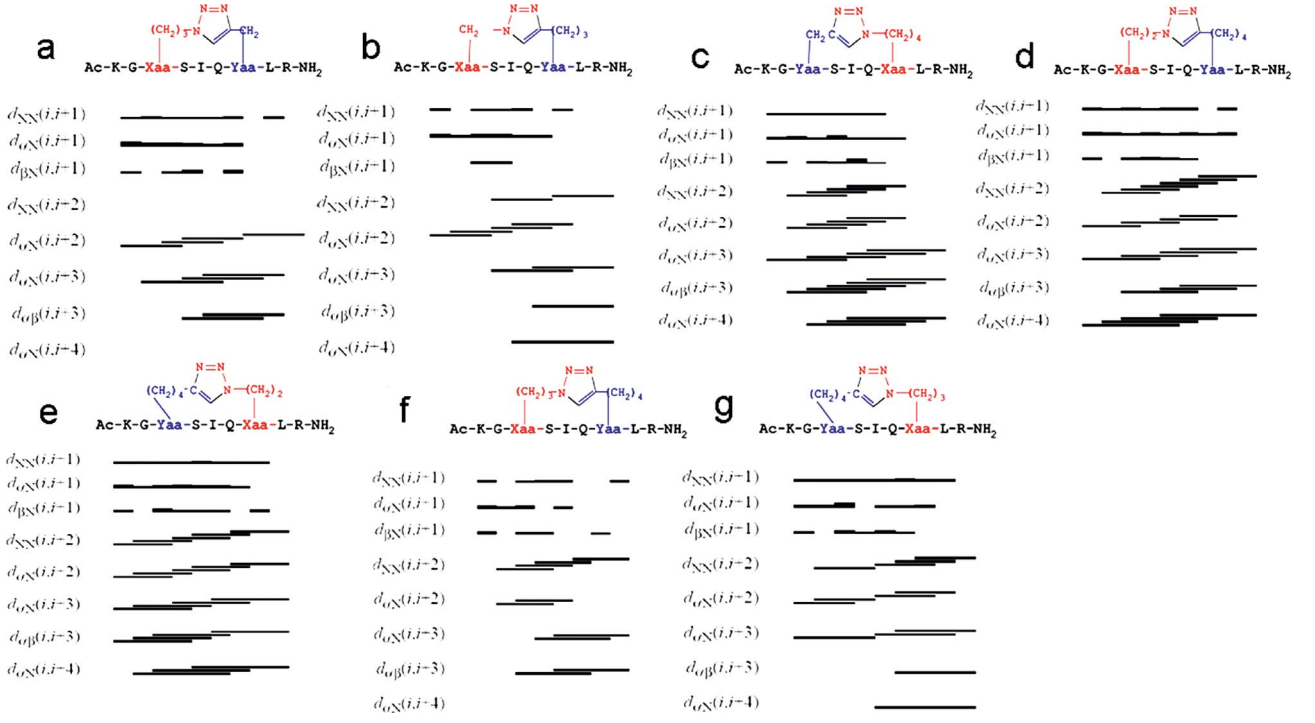

Figure 4. NOE connectivities diagrams of *i*-to-(*i*+4) side-chain-to-side-chain 1,2,3-triazolyl-bridged cyclo-nonapeptide **I**–**II** (panels **a** and **b**) and **IV**–**VIII** (panels **c**–**g**) in water/HFA (1:1 v/v).

NMR Structure Calculations: Three-dimensional structures of cyclo-nonapeptides **I**, **II** and **IV**–**VIII** were calculated by simulated annealing procedures based on sequential and medium-range NOE-derived restraints extracted from NOESY spectra. To avoid overestimation of NOE effects, NOESY spectra were collected using 150, 200, 250 ms mixing times. Interprotonic distances were derived from 200 ms mixing time NOESY spectrum. The best 20 structures out of 50 calculated with the DYANA software package were chosen according to the lowest values of the penalty (f) for the target function. These structures were energy minimized using the distance restraints with a progressively

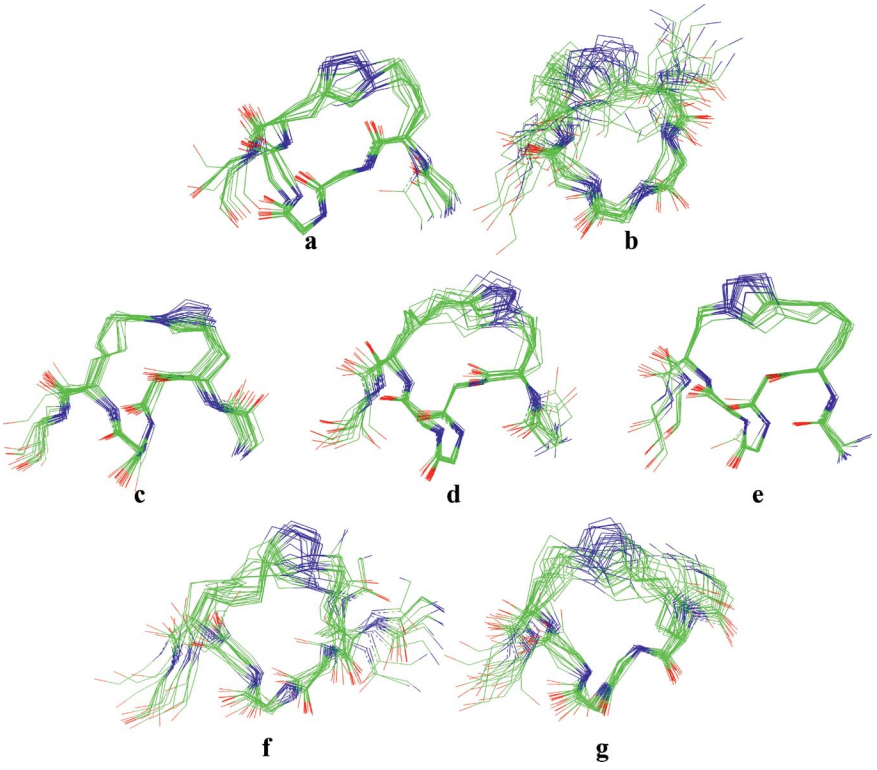

Figure 5. NOESY spectra were collected using 150, 200, 250 ms mixing times. Interprotonic distances were derived from 200 ms mixing time NOESY spectrum. The best 20 structures out of 50 calculated with the DYANA software package were chosen according to the lowest values of the penalty (f) for the target function. These structures were energy minimized using the distance restraints with a progressively smaller force constant. This minimization procedure yielded an improved helical geometry and a lower total energy of the structure.

smaller force constant. This minimization procedure yielded an improved helical geometry and a lower total energy of the structures. Figure 5 shows an all-heavy atom presentation of the bundles of the 20 best DYANA calculated conformers corresponding to cyclo-nonapeptides **I**, **II** and **IV**–**VIII** in water/HFA. The 20 low-energy conformers of each

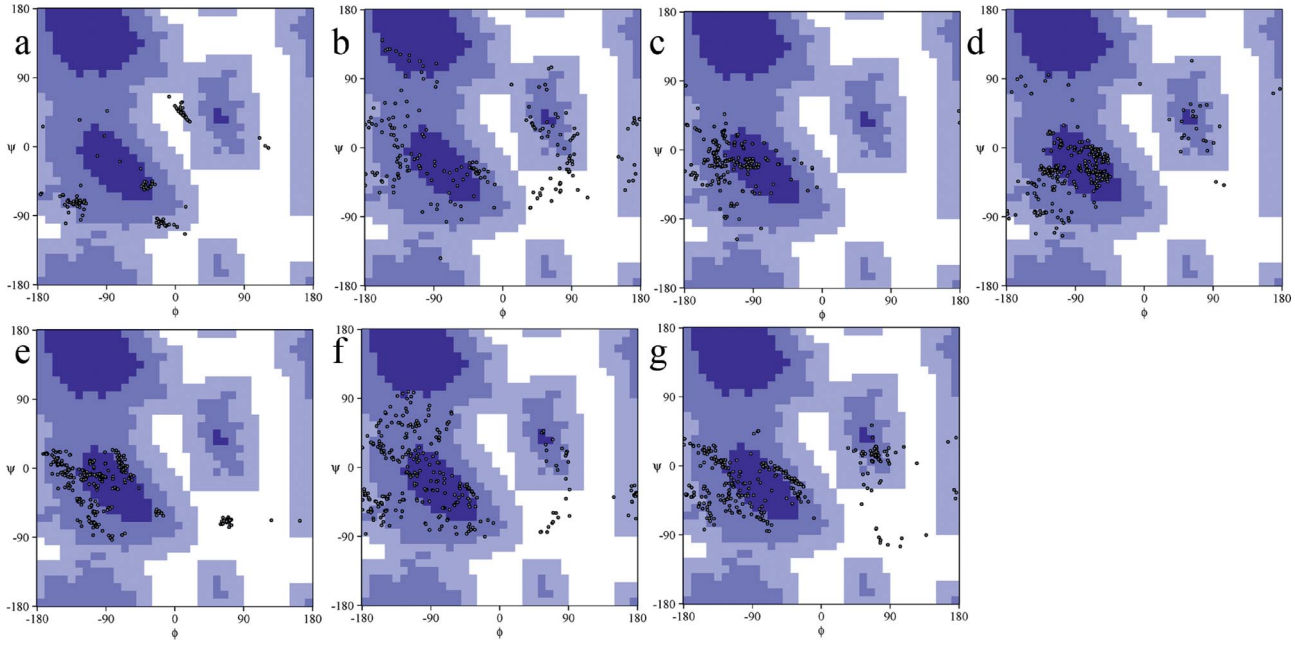

Figure 6. Ramachandran plots of NMR structures of *i*-to-(*i*+4) side-chain-to-side-chain 1,2,3-triazolyl-bridged cyclo-nonapeptides **I**–**II** (panel **a** and **b**) and **IV**–**VIII** (panels **c**–**g**) in water/HFA (1:1, v/v).

cyclo-nonapeptide were overlapped at level of the residues in positions 13 and 17 that carry the side chains involved in the 1,2,3-triazolyl-containing bridge. NMR structure bundles in water/HFA are well-defined, with local displacement of <0.6 Å as calculated for the heavy atoms. Figure 6 shows the Ramachandran plots of NMR structure bundles of the low-energy conformers in water/HFA. A pronounced clustering of dihedral angles is evident, with very few of them located in disallowed regions of the maps.

Conversely, the NMR structure bundles of the cyclo-nonapeptide **I**, **II** and **IV**–**VIII** in water display local displacement of >1.0 Å as calculated for the heavy atoms, confirming the CD data on the presence of disordered structures that are much more flexible than the structures of the same cyclo-nonapeptide in water/HFA. The Ramachandran plots of NMR structure bundles in water display wide scattering of dihedral angles with some of them in disallowed regions (not shown).

NMR Analysis in Water

Analysis of NMR structures in water shows that cyclo-nonapeptides **I**, **V** and **VIII** are characterized by non-regular, disordered conformations. Accordingly, Ramachandran plots show significant scattering of backbone dihedral angles, some of them falling within disallowed regions of the maps. According to PROMOTIF procedure, a weak presence of γ-turns in the Gly[12]-Nva(δ-1-1,2,3-triazolyl)-Ser-Ile[15] segment of cyclo-nonapeptide **I**, and type I β-turn in the Ser[14]-Ile-Gln-Nle[17](δ-4-1,2,3-triazolyl) segment of cyclo-nonapeptide **V** are observed. For cyclo-nonapeptide **VIII** no regular conformation was identified. Ramachandran plots of cyclo-nonapeptides **II**, **IV**, **VI** and **VII** reveals an appreciable presence of γ-turn and β-turn conformations. In particular, according to PROMOTIF analysis, γ- and type I β-turns are found in the C-terminal segment of cyclo-nonapeptide **II** and **IV**, as well as in the Gly[12]-Nle(δ-4-1,2,3-triazolyl)-Ser-Ile[15] and Gly[12]-Nva(δ-1-1,2,3-triazolyl)-Ser-Ile[15] segments of cyclo-nonapeptide **VI** and **VII**, respectively.

NMR Analysis in Water/HFA

Bundles of 20 low-energy conformers representing the backbones of cyclo-nonapetides **I** and **II** are superimposed at the level of Nva[13](δ-1-1,2,3-triazolyl)-Ser-Ile-Gln-Pra[17] and Pra[13]-Ser-Ile-Gln-Nva[17](δ-1-1,2,3-triazolyl) segments, respectively (Scheme 1 and Figure 5, panels **a** and **b**, respectively). The Ramachandran plots show a tight fit of the bundle for cyclo-nonapeptide **I** but not for **II** (Figure 6, panels **a** and **b**, respectively), suggesting that the structure of the former is defined with high precision in the overlapping region, while the structure of the latter is more disordered. Accordingly, the NMR structure-derived bundles show clustering of backbone dihedral angles for cyclo-nonapeptide **I** (Figure 6, panel **a**) and scattering of backbone dihedral angles for cyclo-nonapeptide **II** (Figure 6, panel **b**). For cyclo-nonapeptide **I** several backbone dihedral angles are in disallowed regions suggesting the occurrence of non-regular secondary structures. PROMOTIF analysis of cyclo-nonapeptide **I** confirms these data, by identifying the presence of non-canonical secondary structures. Same analysis of cyclo-nonapeptide **II** confirms a major contribution of disordered structures with a minor presence of γ-turn conformations comprising different triads along the Ser[14]-Ile-Gln-Nva(δ-1-1,2,3-triazolyl)-Leu-Arg[19]-NH_2 sequence.

The bundle formed by superimposition of the 20 low-energy NMR structures of cyclo-nonapeptide **IV** by overlapping the Ser[14]-Ile-Gln-Nle[17](ε-1-1,2,3-triazolyl) segment (Figure 5, panel **c**) reveals a high structural similarity (backbone RMSD ≤ 0.54 Å). The dihedral angles are clustered within allowed regions of the Ramachandran map (Figure 6, panel **c**), indicating the recurrence of regular secondary structures; these, according to PROMOTIF analysis,[25] are identified as regular type II β-turns located at the Gln[16]-Nle(ε-1-1,2,3-triazolyl)-Leu-Arg[19] segment. NMR structure bundles of cyclo-nonapeptide **V** and **VI** (Figure 5, panels **d** and **e**, respectively) display a good overlap of the low-energy conformers at the sequence spanning residues 13 to 17 (RMSD ≤ 0.5). In agreement with these data, a large majority of backbone torsion angles are located within the allowed regions of the Ramachandran plots (Figure 6, panels **d** and **e**), thus confirming the propensity of these cyclo-nonapeptides to assume regular secondary structures. Indeed, PROMOTIF analysis of backbone dihedral angles points to the prevalence of ordered α-helical structures spanning almost the entire sequence Ac-Lys[11]-Gly-hAla(γ-1-1,2,3-triazolyl)-Ser-Ile-Gln-Nle(δ-4-1,2,3-triazolyl)-Leu[18] of cyclo-nonapeptide **V**. Same analysis identifies type I β-turn structures at the Nle[13](δ-4-1,2,3-triazolyl)-Ser-Ile-Gln[16] segment for cyclo-nonapeptide **VI**.

The bundles formed by superimposition of the 20 low-energy NMR structure of cyclo-nonapeptides **VII** and **VIII** by overlapping the Nva[13](δ-1-1,2,3-triazolyl)-Ser-Ile-Gln-Nle[17](δ-4-1,2,3-triazolyl) sequence (Figure 5, panels **f** and **g**) indicate conformational disparity among the calculated structures. Accordingly, in the corresponding Ramachandran maps (Figure 6, panels **f** and **g**), an appreciable scattering of the backbone dihedral angles is evident. PROMOTIF evaluation of the NMR structures of cyclo-nonapeptide **VII**, suggests the presence of α-helical structures spanning the Ac-Lys[11]-Gly-Nva(δ-1-1,2,3-triazolyl)-Ser-Ile-Gln-Nle(δ-4-1,2,3-triazolyl)-Leu[18] segment, with a noticeable presence of type I β-turn in the segment Gln[16]-Nle(δ-4-1,2,3-triazolyl)-Leu-Arg[19]-NH_2. For cyclo-nonapeptide **VIII** a significant presence of γ-turn conformations encompassing the Gly[12]-Nle(δ-4-1,2,3-triazolyl)-Ser-Ile[15] segment is observed. To complete the characterization of the conformational preferences of the cyclo-nonapeptides we analysed the H-bond patterns of the most representative NMR-derived structure for cyclo-nonapeptide **I**, **II** and **IV**–**VIII**. A list of H-bonds involving amino acid backbone, side chains and the 1,2,3-triazolyl ring is reported in Supporting Information (Table S9). H-bonds correlate with the structural regularity of the cyclo-nonapeptides and they involve backbone atoms as well as atoms belonging to the side-chain-to-side-chain bridge that includes the 1,2,3-tri-

azolyl ring. In 1,2,3-triazolyl ring C5-H and N2 play as H bond donor and acceptor respectively.[9,26,27] In cyclo-nonapeptides **I** and **II** C5-H proton of the 1,2,3-triazolyl is H-bond donor to the CO of the backbone of residues 13. However, this pattern does not correspond to any regular secondary structure. In cyclo-nonapeptides **VII** and **VIII** H-bonds involve the backbone atoms with a negligible participation of the 1,2,3-triazolyl-containing bridge. In cyclo-nonapeptides **IV**, **V** and **VI**, regular H-bond patterns involve backbone as well as 1,2,3-triazolyl atoms. C5-H proton is H-bond donor for the CO of the backbone of residues 13 and/or 16, confirming the participation of both non-cyclised and cyclised portions of cyclo-nonapeptides in intramolecular H-bond formation. Interestingly, similar H-bond patterns were reported previously for the cyclo-nonapeptide **III**. Analysis of NOEs involving C5-H proton of the 1,2,3-triazolyl ring, the only 1,2,3-triazolyl atom observed in the proton NMR spectra (see Supporting Information, Table S8), shows that the triazolyl ring is close to the backbone of amino acid residues 13 and 17 participating in the side-chain-to-side-chain cyclization. Moreover, in cyclo-nonapeptides **I**, **II**, **V** and **VII**, C5-H protons are also proximal to protons that do not belong to the bridge, HN and $H_2\beta$ on Ser^{14} or $H_2\gamma$ on Gln^{16}, depending on the orientation of the 1,2,3-triazolyl ring in the bridge, whether it is incorporated in the 1,4- or 4,1-orientation, respectively. In cyclo-nonapeptides **V** C5-H proton of the 1,2,3-triazolyl ring is also in contact with protons that are not included in the cyclic portion, such as Leu^{18} and Arg^{19}. This pattern of interatomic distances, which is dependent on the conformational feature of the cyclopeptide **V**, is similar to that found in the closely related 1,2,3-triazolyl-containing cyclo-nonapeptide **III**.[1] Both cyclo-nonapeptides **III** and **V** share the 1,4-orientation of the 1,2,3-triazolyl ring, which is removed from the C^{α} of residue 13 by more than one methylene.

Discussion

The recently introduced Cu^{I}-catalyzed azide–alkyne 1,3-dipolar Huisgen cycloaddition as a prototypic "click chemistry reaction"[6,8,10] offers the opportunity for introducing the 1,4-disubstituted 1,2,3-triazolyl moiety as a new isoster for peptide bonds.[6,8–13] We postulated that intramolecular side-chain-to-side-chain click reaction between two side chains, one substituted by an ω-azido and the other by an ω-yl function, will generate an heterodetic cyclopeptide that will mimic an analogous lactam-bridged cyclopeptide. Subsequently, we reported the synthesis and conformational analysis of a model *i*-to-(*i*+4) side-chain-to-side-chain 1,4-disubstituted 1,2,3-triazolyl-bridged cyclo-nonapeptide **III** (Scheme 1) structurally related to the helical *i*-to-(*i*+4) lactam-bridged cyclopeptide [Lys^{13}(&^{1}),Asp^{17}(&^{2})]PTHrP(1–34)NH_2.[1] Our current study aims to systematically explore the relationship between the features of the *i*-to-(*i*+4) intramolecular bridge containing the 1,4-disubstituted 1,2,3-triazolyl moiety, as it relates to the size of the bridge and the location and orientation of the 1,2,3-triazolyl moiety within the bridge, and the conformational propensities of the heterodetic cyclo-nonapeptides **I**–**II** and **IV**–**VIII** (Scheme 1).

Combination of stepwise solid-phase assembly of the linear peptide, Fmoc/*t*Bu strategy employing preformed ω-azido- and ω-yl-modified N^{α}-Fmoc-protected amino acids, and solution phase Cu^{I}-catalyzed click reactions of the purified linear peptide resulted in good yields of the heterodetic 1,2,3-triazolyl-bridged cyclo-nonapeptides. As anticipated, in the absence of catalyst intramolecular cyclization and oligomerization are negligible. The CD and NMR measurements of the cyclo-nonapeptides **I**–**VIII** were carried out in water and water/HFA mixture. Water is considered the most bio-compatible medium to perform solution-phase conformational studies since it is the predominant component of most biological compartments. Nevertheless, water solutions enhance the conformational flexibility of short peptides compromising the collection of a sufficient number of NOE-based interprotonic distances needed for 3D-model building. Therefore, in order to enhance the prevalence of ordered, compact and relevant conformers over extended and/or disordered and biologically irrelevant ones, water-cosolvent mixtures with a viscosity higher than that of pure water are frequently used.[28] Mixtures of water with fluorinated cosolvents such as water/trifluoroethanol (TFE), water/HFA and water/hexafluoroisopropyl alcohol (HFIP), are frequently used as media to induce "environmental constraints" in peptides.[29] Fluorinated cosolvents exert a helix inducing/stabilizing effect, which does not override the intrinsic conformational tendency dictated by the specific sequence.[28,30,31] In addition, these mixtures are compatible with NMR experiments, allowing measurements of the same samples in both CD and NMR and subsequently obtaining compatible data.

Analysis of CD spectra suggests that in water, heterodetic cyclo-nonapeptides **I**–**II** and **IV**–**VIII** present different ensembles of turn-helical conformers presented in different proportions. This finding is diagnostic of the flexibility of the cyclo-nonapeptides in water. Confirming the CD data, NOESY spectra in water contain NOEs suggesting the formation of only incipient turn-helical conformations, which are insufficient to calculate high resolution 3D models of cyclo-nonapeptides **I**–**II** and **IV**–**VIII**. CD data in water/HFA mixture show a dramatic decrease of turn and random coil conformations and point to a high prevalence of helical structures. Accordingly, high quality NMR structures were calculated on the basis of NOE data in HFA/water. In any event, by comparing the incipient conformational tendency of cyclo-nonapetides in water and in HFA/water a general agreement seems to exist between the two sets of structural data, thus supporting the contention that water/HFA is a suitable solvent system to enhance and stabilize, but not to override the intrinsic conformational propensities of peptides. The comparison of the conformational features of the cyclo-nonapeptides in water/HFA mixture indicates that: 1) cyclo-nonaopeptide **I**, in which the 1,2,3-triazolyl moiety is flanked by chains comprised of a total of 4 methylene groups $(CH_2)_{(m+n=4)}$ (Scheme 1), forms a well defined con-

formational ensemble that does not correspond to any canonical secondary structure (Figure 6, panel **a**); 2) cyclo-nonapeptides **IV/VI**, which contain bridges comprised of a total of 5 and 6 methylene groups $(CH_2)_{(m+n = 5 \text{ and } 6)}$ (Scheme 1), are characterized by ordered and regular secondary structures (Figure 5, panels **c**–**e**); and 3) cyclo-nonapeptides **II**, **VII** and **VIII**, in which the 1,2,3-triazolyl moiety is flanked by chains comprised of a total of 4 and 7 methylene groups $(CH_2)_{(m+n = 4 \text{ and } 7)}$ (Scheme 1), form a wide spread of low-energy conformations (Figure 5, panels **b**, **f** and **g**). These results suggest that *i*-to-(*i*+4) side-chain-to-side-chain 1,2,3-triazolyl-bridged cyclo-nonapeptides comprised of bridges containing a total of 4 and 7 methylene groups tend to form either non-canonical (cyclo-nonapeptide **I**) or disordered (cyclo-nonapeptides **II**, **VII** and **VIII**) secondary structures. Apparently, cyclo-nonapeptides constrained by a smaller bridge containing a total of only 4 methylens will be forced into either a stable non-regular structure or fail to form a tight ensemble of closely related conformations (cyclo-nonapeptides **I** and **II**, respectively). At the same time, cyclo-nonapeptides linked by a larger bridge that contains a total of 7 CH_2 groups will entertain larger molecular flexibility and will form a divergent ensemble of non-regular conformations (cyclo-nonapeptides **VII** and **VIII**). Evidently, cyclo-nonapeptides **IV/VI**, which are cyclized through bridges containing a total of 5 and 6 CH_2 groups, represent the optimal size to assume regular secondary structures. Similar to cyclo-nonapeptides **IV/VI**, the conformational analysis of the previously reported cyclo-nonapeptide **III**, containing a total of 5 CH_2 groups in the 1,2,3-triazolyl containing bridge, revealed formation of a well defined canonical structure.[1] The comparison of low-energy 3D models of cyclo-nonapeptides **IV/VI** clarify the role of the location of the 1,2,3-triazolyl moiety within the bridge on the stabilization of the conformational propensities of the cyclopeptides. The close proximity of the 4,1-disubstituted 1,2,3-triazolyl ring to the backbone in cyclo-nonapeptide **IV** explains the constraints imposed on the proximal sequence Gly^{12}-Ala(β-4-1,2,3-triazolyl)-Ser^{14} leading to a slight distortion from a canonical conformation. In this compound, there is a particular structural effect related to the presence of Ser^{14} γ-OH. The separation between the Cα of residue 13 and the 1,2,3-triazolyl ring by only one methylene induces the distortion of α-helical torsion angles due to a favourable dipolar interaction between Ser^{14} γ-OH and triazolyl ring N2. Conversely, in the same cyclo-nonapeptide the longer chain of 4 CH_2 groups separating the 1,2,3-triazolyl ring from the Cα of residue 17 allows the Gln^{16}-Nle(ε-1-1,2,3-triazolyl)-Leu^{18} to assume a much greater structural regularity than that of the preceding sequence. Interestingly, the structural distortion observed in cyclopetide **IV** is not evident in the related cyclopeptide **III** both have a total of 5 CH_2 groups in the bridge formed by combinations of either 1+4 or 4+1 CH_2 groups flaking the 4,1- and 1,4-(1,2,3-triazolyl) moiety, respectively. In cyclo-nonapeptide **III** the contacts between the 1,2,3-triazolyl ring and the backbone in Gln^{16}-Ala(β-4-1,2,3-triazolyl)-Leu^{18} do not interfere with the regularity of the backbone structure. In the absence of this structural constraint, cyclo-nonapeptides **V** and **VI**, in which the total number of CH_2 groups in the 1,2,3-triazolyl-containing bridge is greater than in cyclo-nonapeptide **IV** (6 vs. 5) and the number of the CH_2 groups in the chains flanking the 1,2,3-triazolyl ring is always greater than 1, assume regular conformations that span the full sequence. These canonical conformations form regardless the 1,4- or 4,1-orientation of the 1,2,3-triazolyl moiety in respective cyclo-nonapeptides **V** and **VI**. This optimized structural regularity of cyclopeptides **V** and **VI** is also reflected in their extensive H-bonds patterns where the participation of backbone as well as 1,2,3-triazolyl ring atoms is evident. Comparison of the low-energy conformations of heterodetic 1,2,3-triazolyl-containing cyclo-nonapeptides **IV**–**VI** with either the previously reported low-energy conformation of the parent α-helical *i*-to-(*i*+4) lactam-bridged cyclo-nonapeptide **1** (Figure 7) or its isosteric 1,2,3-triazolyl-containing cyclo-nonapeptide **III** (Figure 8) reveals remarkable structural similarities.[1] Pairwise superposition of the backbone heavy atoms of Xaa^{13}-Ser-Ile-Gln-Yaa^{17} sequences of the low-energy NMR conformers of cyclo-nonapeptides **IV**–**VI** with either the lactam **1** or the homologous cyclo-nonapeptide **III** reveals RMSD$<$0.8 Å. In particular, the best structural overlap is observed for cyclo-nonapetides **V** and **VI**. For these conformers the overlapping with the corresponding segments of lactam **1** (Figure 7, panels **b** and **c**) and cyclopeptide **III** (Figure 8, panels **b** and **c**) shows RMSD$<$0.1, which is extended to include the methylene chain of the bridging portion. In Figures 7 and 8 the orientation of the side chains of the residues included in the cyclic portions of cyclo-nonapetides **IV**, **V** and **VI** are compared to the corresponding side chains of lactam **1** and the homologous cyclo-nonapeptide **III**, respectively. We observe good overlap of Ser^{14}, Gln^{15} and Ile^{16} side chains located within the cyclic portion for each pair of conformers analysed. We anticipate that in addition to the requirements for specific side chains disposition different macromolecular targets will differentially accommodate the various orientations of the 1,2,3-triazolyl rings present in the *i*-to-(*i*+4) bridge. Taken all together, our study suggest that heterodetic 1,4- or 4,1-disubstituted 1,2,3-triazolyl-bridged cyclo-nonapeptides obtained via *i*-to-(*i*+4) side-chain-to-side-chain cyclization can be successfully designed to reproduce and stabilize α-helical conformations. Bridges containing 1,2,3-triazolyl moieties flanked by stretches of $(CH_2)_{(m = 1,2, \text{ and } 4)}$ and $(CH_2)_{(n = 1,2, \text{ and } 4)}$ where $m+n$ = 5 or 6 will nicely accommodate α-helical structures.

Moreover, the larger bridges containing a total of 6 CH_2 groups formed by flanking the 1,2,3-triazolyl ring between chains of 2 and 4 CH_2 groups, as in cyclo-nonapeptides **V** and **VI**, will accommodate the triazolyl ring without imposing any destabilizing spatial interactions with the backbone leading to larger propensity for ordered structures. These conformationally favoured cyclo-nonapeptides **V** and **VI** show great conformational similarity with the helical model lactam-bridged cyclo-nonapeptide **1** and with its isosteric heterodetic 1,2,3-triazolyl-containing cyclo-nonapep-

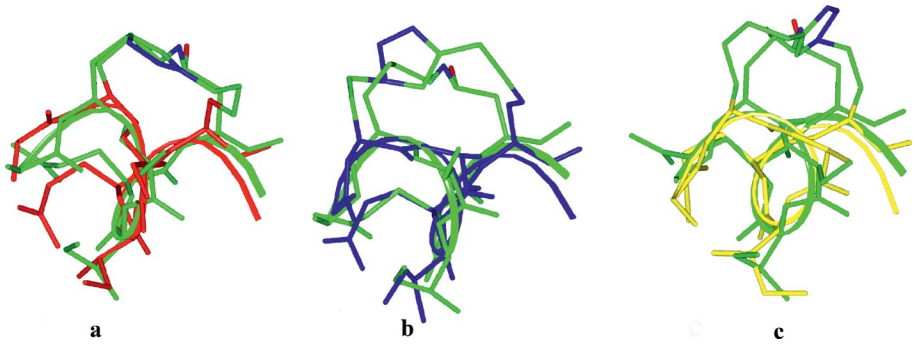

Figure 7. Superposition of low-energy NMR conformers of the heterodetic 1,2,3-triazolyl containing cyclo-nonapeptides **IV**, **V**, and **VI** (**a**, **b**, and **c**, respectively) with low-energy NMR conformer of isosteric lactam-bridged cyclo-nonapeptide **1**. The backbone of cyclo-nonapeptides **1** is colored in green and those of the clicked cyclo-nonapeptides **IV**, **V** and **VI** are coloured in red, blue and yellow, respectively. In all cyclo-nonapetides the bridged side chains are colour-coded by atom types (C: green; N: blue; and O: red).

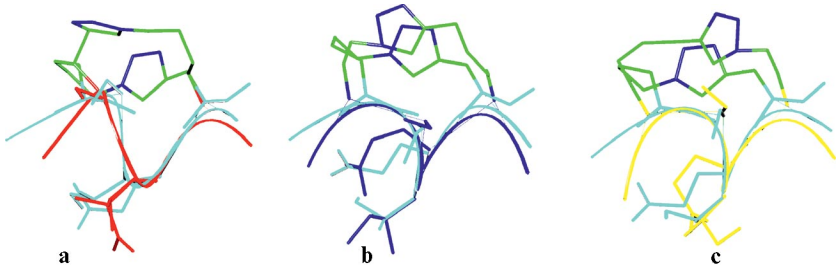

Figure 8. Superposition of low-energy NMR conformers of the heterodetic 1,2,3-triazolyl-containing cyclo-nonapeptides **IV**, **V**, and **VI** (**a**, **b** and **c**, repectively) with low-energy NMR conformer of the homologous 1,2,3-triazolyl-containing cyclo-nonapeptide **III**. Side chains of the macrocycle forming sequence Ser^{14}-Gln-Ile^{16} are dispayed in stick rendering. Backbone of clicked cyclo-nonapeptides **III**–**VI** are colour-coded in white, red, blue and yellow, respectively. In all clicked cyclo-nonapeptides the bridged side chains are colour-coded by atom types (C: green and N: blue).

tide **III**. Importantly, our studies suggest that the *i*-to-(*i*+4) side-chain-to-side-chain 1,4- and 4,1-disubstituted 1,2,3-triazolyl-bridged cyclo-nonapeptide, in addition to successfully reproducing the α-helical structure, can be fine tuned to support a wide range of distorted and non-canonical structures. Future studies conducted in our laboratories will provide additional insight on the relationship between conformation and the separation between residues participating in the side-chain-to-side-chain cyclization, size of the connecting bridge, position of the 1,2,3-triazolyl ring in the bridge and last but not least, the orientation of the triazolyl ring in the bridge.

Experimental Section

Materials: 9-Fluorenylmethyloxycarbonyl (Fmoc)-protected L-amino acids and Rink amide resin (0.63 mmol g^{-1}) were obtained from Novabiochem AG (Laufelfingen, Switzerland). 2-(1*H*-Benzotriazol-1-yl)-1,1,3,3-tetramethyluronium tetrafluoroborate (TBTU), *N*-Hydroxybenzotriazole (HOBt) were purchased from Iris-Biotech. Peptide-synthesis grade *N*,*N*-dimethylformamide (DMF) was purchased from Scharlau (Barcelona, Spain). Trifluoroacetic acid (TFA), dichloromethane (DCM), piperidine, acetic anhydride (Ac_2O), and *N*-methylmorpholine (NMM) were purchased from Aldrich. High performance liquid chromatography (HPLC)-grade acetonitrile (MeCN) was purchased from Carlo–Erba (Italy).

Synthesis of N^{α}-Fmoc-Xaa(ω-N_3)-OH and N^{α}-Fmoc-Yaa(ω-yl)-OH: The detailed syntheses of these alkynyl- and azido-containing building blocks are described elsewhere.[16]

Solid Phase Synthesis of Ac[Xaa^{13}(ω-N_3),Yaa^{17}(ω-yl)]hPTHrP(11–19)NH_2 (I′, V′ and VII′) and Ac[Yaa^{13}(ω-yl),Xaa^{17}(ω-N_3)]hPTHrP(11–19)NH_2 (II′,IV′,VI′ and VIII′)

Synthesis of Rink amide resin-bound Ac[Lys^{11}(N^{ε}-Boc),Xaa^{13}(ω-N_3),Ser^{14}(*t*Bu),Gln^{16}(Trt),Yaa^{17}(ω-yl),Arg^{19}(N^{G}-Pbf)]hPTHrP(11–19) and Ac[Lys^{11}(N^{ε}-Boc),Yaa^{13}(ω-yl),Ser^{14}(*t*Bu),Gln^{16}(Trt),Xaa^{17}-(ω-N_3),Arg^{19}(N^{G}-Pbf)]hPTHrP (11–19).

Peptides **I′**–**VIII′** were synthesized on a manual batch synthesizer (PLS 4×4, Advanced ChemTech) using a Teflon reactor (10 mL), applying the Fmoc/*t*Bu solid phase peptide synthesis (SPPS) procedure. The N^{α}-Fmoc-Arg(N^{G}-pbf)-Rink amide resin was swelled with DMF (1 mL/100 mg of resin) for 20 min before use.

Stepwise peptide assembly was performed by repeating for each added amino acid the following deprotection-coupling cycle: 1) Swelling: DMF (1 mL/100 mg of resin) for 5 min; 2) Fmoc-deprotection: resin is washed twice with 20% piperidine in DMF (1 mL/100 mg of resin, one wash for 5 min followed by another wash for 20 min); 3) Resin washings: DMF (3×5 min); 4) Coupling: scale employing TBTU/HOBt/NMM (2.5:2.5:3.5 equiv.) as

the coupling system and 2.5 equiv. of the Fmoc protected amino acids, except for Xaa(ω-N_3) and Yaa(ω-yl) (1.5 equiv.), in DMF (1 mL/100 mg of resin) for 40 min. Each coupling was monitored by Kaiser test[32] and was negative, therefore recouplings were not needed; 5) Resin washings: DMF (3 × 5 min) and DCM (1 × 5 min).

Amino Terminal Acetylation. General Procedure: The free *N*-terminal α-amino of the resin-bound peptides was acetylated by two consecutive steps. A 30 min exposure to Ac_2O/NMM in DCM (20 equiv. 1.6 mL of DCM) was followed by a additional 1.5 h treatment with a fresh acetylation mixture. The reaction was monitored by Kaiser test.[32]

Deprotection, Cleavage and Purification of Free Peptide. General Procedure: Peptides cleavage from the resin and simultaneous deprotection of the amino acid side chains were carried out with a mixture of TFA/anisole/1,2-ethanedithiol/phenol/H_2O (94:1:1:1:1 v/v/v/v/v, 1 mL/100 mg of resin-bound peptide). The cleavage was carried out for 3 h with vigorously shaking at room temperature. Resins were filtered and washed with TFA. The filtrate was concentrated under N_2 stream, addition of cold diethyl ether resulted in a precipitate that was separated by centrifugation, dissolved in H_2O and lyophilized on an Edwards apparatus, model Modulyo.

Peptides were purified by semipreparative RP-HPLC on a Waters 600 equipped with Jupiter C18 (10 μm, 250 × 10 mm), at a flow rate of 4 mL/min employing a linear gradient 10% to 60% of B in A in 20 min were the solvent system used was A = 0.1% TFA in H_2O and B = 0.1% TFA in CH_3CN. Fractions were analyzed by ACQUITY UPLC (Waters Corporation, Milford, Massachusets) coupled to a single quadrupole ESCI-MS (Micromass ZQ) using an ACQUITY BEH C18 column (1.7 μm, 2.1 × 50 mm) at 30 °C, with a flow rate of 0.45 mL/min employing a linear gradient of 10% to 60% of B in A in 3 min (A and B are the same as above).

Solution phase Cu^I-catalyzed intramolecular azide–alkyne 1,3-dipolar Huisgen cycloaddition: Synthesis of Ac[$Xaa^{13}(^1)$,$Yaa^{17}(^2)$]-hPTHrP(11–19)NH_2[{&^{1}$(CH_2)_{(n = 2 and 3)}$-1,4-(1,2,3)triazolyl-$(CH_2)_{(n = 1 and 4)}$&^{2}}] (**I**, **V** and **VII**) and Ac[$Yaa^{13}(^1)$,$Xaa^{17}(^2)$]-hPTHrP(11–19)NH_2[{&^{1}$(CH_2)_{(n = 1 and 4)}$-4,1-(1,2,3)triazolyl-$(CH_2)_{(n = 2–4)}$&^{2}}] (**II**, **IV**, **VI** and **VIII**).

Cyclization of Ac[Xaa^{13}(ω-N_3),Yaa^{17}(ω-yl)]hPTHrP(11–19)NH_2 (**I′**, **V′** and **VII′**) and Ac[Yaa^{13}(ω-yl),Xaa^{17}(ω-N_3)]hPTHrP(11–19)-NH_2 (**II′**,**IV′**,**VI′** and **VIII′**).

To a solution of the linear peptide (3.1 μmol) in H_2O/*t*BuOH (4 mL, 2:1 v/v) were added $CuSO_4$·$5H_2O$ (43.4 μmol) and ascorbic acid (40.3 μmol). The mixture was stirred overnight at room temperature, concentrated and lyophilized. The crude heterodetic cyclo-nonapeptides were purified (≥ 97% purity) by RP-18 column LiChroprep employing the same solvent system as mentioned above.

Circular Dichroism Spectroscopy: All CD spectra were recorded on a Jasco J-810 spectropolarimeter using cells of 1 mm path length. The pH of the samples was adjusted to 6.6 with aqueous phosphate buffer (100 mM, pH 7.2). After pH adjustment, samples were lyophilized and dissolved in water, or in water containing 50% (v/v) hexafluoroacetone (HFA) to obtain a peptide concentration of 0.02 mM. Spectra were the average of two scans from 190 to 260 nm, recorded with a band width of 0.5 nm at scan rate of 5 nm/min.

For estimation of secondary structure content, CD spectra were analyzed using CONTINN algorithm of DICHROWEB on-line server.[18]

NMR Spectrometry: Samples were prepared by dissolving about 1.2 mg of the heterodetic 1,2,3-triazolyl-containing cyclo-nonapeptides in 0.5 mL of aqueous phosphate buffer (pH 6.6, 100 mM). To prepare samples for measurements in water/HFA, the samples in aqueous phosphate buffer were lyophilized and dissolved in a mixture of water/HFA (0.5 mL, 1:1, v/v). NMR spectra were recorded on a Bruker DRX-600 spectrometer. One-dimensional (1D) NMR spectra were recorded in the Fourier mode with quadrature detection. The water signal was suppressed by a low-power selective irradiation in the homogated mode. Double Quantum- Filtered Correlation Spectroscopy (DQF-COSY), Total Correlated Spectroscopy (TOCSY) and Nuclear Overhauser Effect Spectroscopy (NOESY)[19–21] experiments were run in the phase-sensitive mode using quadrature detection in ω1 by time-proportional phase incrementation of the initial pulse.[33] Data block sizes comprised of 2048 addresses in *t*2 and 512 equidistant *t*1 values. Before Fourier transformation, the time domain data matrices were multiplied by shifted $\sin^2$ functions in both dimensions. A mixing time of 70 ms was used for the TOCSY experiments. NOESY experiments were run at 300 K with mixing times in the range of 100–250 ms. The qualitative and quantitative analyses of DQF-COSY, TOCSY and NOESY spectra were obtained using the SPARKY[22] interactive program package. Complete proton resonance assignments were achieved with the Wüthrich procedure.[23]

NMR Structure Calculation: Sequential and medium range NOE-derived distances were used to generate 3D models of the heterodetic 1,2,3-triazolyl-containing cyclo-nonapeptides. These structures were subjected to simulated annealing procedure using the DYANA software package[34] and energy minimized with the SANDER module of the AMBER 5 program[35] using for first 1000 steps the steepest descent method and for the following 4000 steps the conjugate gradient method. A non-bonded cut-off of 12 Å and a distance-dependent dielectric term ($e = 4 \cdot r$) were used. The minimization protocol included three steps in which NOE-derived distances were used as constraints with a force constant, of 1000, 100 and 10 kcal/mol Å, respectively. The final *pdb* files were analyzed and validated using PROMOTIF software.[25]

Molecular Dynamics: Molecular dynamics runs were performed using the SANDER module of the AMBER 5 software at a constant temperature of 300 K, using a non-bonded cut-off of 12 Å and a distance-dependent dielectric term ($e = 4 \cdot r$). NMR mean structures of the heterodetic 1,2,3-triazoyl-containing cyclo-nonapeptides were chosen as starting structures. The molecular dynamics simulations were performed with a rather drastic limitation of allowed movements for backbone atoms whereas side-chain atoms were allowed to move according to a small value of force constant restraints. A force constant of 1000 kcal/mol Å was applied on the NOE derived distance restraints of the backbone atoms, whereas a force constant of 10 kcal/mol Å was used to constrain side-chain atoms. Heating the system for 1 ps and 10 ps of initialization time was followed by 500 ps simulation with 1 fs time steps. Structures were saved every 5 ps. The average AMBER energy was 1180 kcal/mol for the 1,2,3-triazolyl-containing cyclo-nonapeptides. The all atoms root mean square deviation (RMSD) from the start of the trajectory was 1.25 Å for the 1,2,3-triazolyl-containing cyclo-nonapeptides. The final structures were analyzed using the Insight 98.0 program (Molecular Simulations, San Diego, CA).

Supporting Information (see also the footnote on the first page of this article): HPLC tracing and MS of the linear precursors and cyclo-nonapeptides **I**–**II** and **IV**–**VIII**; Proton Chemical Shifts of clicked cyclo-nonapeptides I–**II** and **IV**–**VIII** in water and water/HFA. Amide and fingerprint regions of NOESY spectra for clicked

cyclo-nonapeptides **I**–**II** and **IV**–**VIII** in water and water/HFA. Interatomic distances involving triazolyl C5 proton in clicked cyclo-nonapeptides **I**–**II** and **V**–**VIII**. Hydrogen bonds observed in the low-energy NMR structures.

[1] S. Cantel, C. Isaad Ale, M. Scrima, J. J. Levy, R. D. DiMarchi, P. Rovero, J. A. Halperin, A. M. D'Ursi, A. M. Papini, M. Chorev, *J. Org. Chem.* **2008**, *73*, 5663–5674.

[2] J. Rivier, G. Kupryszewski, J. Varga, J. Porter, C. Rivier, M. Perrin, A. Hagler, S. Struthers, A. Corrigan, W. Vale, *J. Med. Chem.* **1988**, *31*, 677–682.

[3] J. Rizo, L. M. Gierasch, *Annu. Rev. Biochem.* **1992**, *61*, 387–418.

[4] C. Schafmeister, J. Po, G. Verdine, *J. Am. Chem. Soc.* **2000**, *122*, 5891–5892.

[5] A. Felix, E. Heimer, C. Wang, T. Lambros, A. Fournier, T. Mowles, S. Maines, R. Campbell, B. Wegrzynski, V. Toome, *Int. J. Pept. Prot. Res.* **1988**, *32*, 441–454.

[6] C. W. Tornoe, C. Christensen, M. Meldal, *J. Org. Chem.* **2002**, *67*, 3057–3064.

[7] M. Meldal, C. W. Tornoe, *Chem. Rev.* **2008**, *108*, 2952–3015.

[8] V. V. Rostovtsev, L. G. Green, V. V. Fokin, K. B. Sharpless, *Angew. Chem. Int. Ed.* **2002**, *41*, 2596–2599.

[9] C. W. Tornoe, S. J. Sanderson, J. C. Mottram, G. H. Coombs, M. Meldal, *J. Comb. Chem.* **2004**, *6*, 312–324.

[10] H. C. Kolb, K. B. Sharpless, *Drug Discov. Today* **2003**, *8*, 1128–1137.

[11] W. S. Horne, M. K. Yadav, C. D. Stout, M. R. Ghadiri, *J. Am. Chem. Soc.* **2004**, *126*, 15366–15367.

[12] A. Brik, J. Alexandratos, Y. C. Lin, J. H. Elder, A. J. Olson, A. Wlodawer, D. S. Goodsell, C. H. Wong, *Chembiochem* **2005**, *6*, 1167–1169.

[13] V. D. Bock, D. Speijer, H. Hiemstra, J. H. van Maarseveen, *Org. Biomol. Chem.* **2007**, *5*, 971–975.

[14] M. Chorev, E. Roubini, R. L. McKee, S. W. Gibbons, M. E. Goldman, M. P. Caulfield, M. Rosenblatt, *Biochemistry* **1991**, *30*, 5968–5974.

[15] S. Maretto, S. Mammi, E. Bissacco, E. Peggion, A. Bisello, M. Rosenblatt, M. Chorev, D. F. Mierke, *Biochemistry* **1997**, *36*, 3300–3307.

[16] A. Le Chevalier Isaad, F. Barbetti, P. Rovero, A. D'Ursi, M. Chelli, M. Chorev, A. Papini, *Eur. J. Org. Chem.* **2008**, *31*, 5308–5314.

[17] T. Hu, R. Tannert, H. Arndt, H. Waldmann, *Chem. Commun.* **2007**, 3942–3944.

[18] L. Whitmore, B. Wallace, *Nucleic Acids Res.* **2004**, *32*, W668.

[19] A. Bax, D. Davis, *J. Magn. Reson.* **1985**, *65*, 355–360.

[20] U. Piantini, O. Sorensen, R. Ernst, *J. Am. Chem. Soc.* **1982**, *104*, 6800–6801.

[21] J. Jeener, B. Meier, P. Bachmann, R. Ernst, *J. Chem. Phys.* **1979**, *71*, 4546.

[22] T. Goddard, D. Kneller, University of California, San Francisco, **2004**.

[23] K. Wüthrich, *NMR of Proteins and Nucleic Acids*, Wiley Interscience, **1986**.

[24] D. Wishart, B. Sykes, *J. Biom. NMR* **1994**, *4*, 171–180.

[25] E. G. Hutchinson, J. M. Thornton, *Protein Sci.* **1996**, *5*, 212–220.

[26] Y. Bourne, H. C. Kolb, Z. Radic, K. B. Sharpless, P. Taylor, P. Marchot, *Proc. Natl. Acad. Sci. USA* **2004**, *101*, 1449–1454.

[27] M. Whiting, J. Muldoon, Y. C. Lin, S. M. Silverman, W. Lindstrom, A. J. Olson, H. C. Kolb, M. G. Finn, K. B. Sharpless, J. H. Elder, V. V. Fokin, *Angew. Chem. Int. Ed.* **2006**, *45*, 1435–1439.

[28] R. Rajan, S. Awasthi, S. Bhattacharjya, P. Balaram, *Biopolymers* **1997**, *42*, 125–128.

[29] D. Picone, A. D'Ursi, A. Motta, T. Tancredi, P. Temussi, *Eur. J. Biochem.* **1990**, *192*, 433–439.

[30] K. Shiraki, K. Nishikawa, Y. Goto, *J. Mol. Biol.* **1995**, *245*, 180.

[31] F. D. Sonnichsen, J. E. Van Eyk, R. S. Hodges, B. D. Sykes, *Biochemistry* **1992**, *31*, 8790–8798.

[32] E. Kaiser, R. Colescott, C. Bossinger, P. Cook, *Anal. Biochem.* **1970**, *34*, 595–598.

[33] D. Marion, K. Wüthrich, *Biochem. Biophys. Res. Commun.* **1983**, *113*, 967.

[34] P. Guntert, C. Mumenthaler, K. Wuthrich, *J. Mol. Biol.* **1997**, *273*, 283–298.

[35] D. Case, D. Pearlman, J. Caldwell, T. Cheatham III, W. Ross, C. Simmerling, T. Darden, K. Merz, R. Stanton, A. Cheng, University of California, San Francisco, **1997**.

Received: October 14, 2009
Published Online: December 16, 2009

